

INDUCTION MELTING IN COLD CRUCIBLE FURNACE FOR THE PRODUCTION OF COMPONENTS IN TURBINE APPLICATIONS

*M. Guglielmi*¹, *E. Baake*¹, *A. Koppen*¹, *E. Holzmann*², *S. Herbst*²

¹ *Institute of Electrotechnology, Leibniz University Hannover,
Wilhelm-Busch-Strasse 4, 30167 Hanover, Germany*

² *Institut für Werkstoffkunde, Leibniz University Hannover,
An der Universität 2, 30823 Hanover, Germany*

In the last two decades, the interest towards Nb-MASC, (*i.e.* niobium-Metal And Silicide Composite) alloys has grown significantly because of their promising mechanical properties. Their tolerance to high temperatures drove much research aimed at the production of components operating in severe environments, in particular, blades of turbines for land and aircraft applications. However, the manufacture of Nb-MASC alloys still encounters multiple challenges, primarily stemming from the chemical reactivity of liquid niobium and the frequent non-homogeneity of the solid cast. To overcome such complications, this work proposed the employment of induction melting in the cold crucible furnace. It was demonstrated that a binary Nb-18Si compound could be alloyed with excellent homogeneity using a single melt under vacuum atmosphere. On the other hand, a six-component Nb-16Si-22Ti-4Cr-3Al-2Hf compound required multiple melting steps of the same sample and argon atmosphere to obtain satisfactory homogeneity of the cast. In general terms, this work demonstrates the induction cold crucible furnace to be an energy-efficient solution for the manufacture of highly homogeneous samples on a laboratory scale and a valuable alternative to the alloying strategies employed until now.

Introduction.

The growing level of CO₂ and NO_x emissions from the fields of aviation and energy production is prompting stricter global regulations and a urgent need to reduce the carbon footprint associated with fossil fuel combustion. Reduction of fuel consumption is one of the obligatory steps on the way to the technological improvement of the turbines used for aircraft and land applications.

The efficiency of turbines is influenced by two main factors: their weight and maximum operating temperatures. Consequently, there is a growing demand for the development of advanced materials that are not only lighter and mechanically stronger but also capable of maintaining structural integrity and performance under high-temperature conditions. Achieving these goals necessitates the exploration of novel materials and manufacturing techniques that can optimize both thermal and mechanical properties, ensuring greater fuel efficiency and reduced environmental impact in high-performance turbine applications [1].

As blades are typically the limiting components of gas turbines because are constantly stressed by vibrations and extreme temperatures, their current production is realized with Ni-based (*i.e.* nickel-based) superalloys. These stand out mostly for their excellent creep behaviour and corrosion resistance but are limited by their high mass density (8.15–8.35 g/cm³) and maximum operating temperature of 1150°C. At the actual state, superalloys reached their technological limits and cannot withstand a further temperature increase.

The need for materials with superior mechanical properties is spurring intense research in the field of refractory metals. Above all, the best candidates to replace the Ni-

based superalloys are the so-called Nb-MASC (Metal And Silicide Composites), which have the potential to enhance the efficiency of the turbines with a tolerable operating temperatures of 1350°C, low density, in the range of 6.6–7.2 g/cm³, and mechanical properties comparable to the ones of superalloys [2–4]. Complementary properties like oxidation resistance and creep behaviour are enhanced with a minor addition of other elements like aluminium (Al), titanium (Ti), chromium (Cr) and hafnium (Hf) [5].

1. State of the art and investigation approach.

Despite this set of promising advantages, a controlled manufacturing of the Nb-MASC alloys is technically challenging: their melting point over 1750°C and their chemical reactivity make the employment of ceramic or graphite-based crucibles practically impossible. In addition, Nb-MASC alloys suffer from strong inhomogeneities due to the presence of multiple elemental components with highly dissimilar physical properties [6]. This naturally compromises the quality of the solidified cast, considering that the chemical concentration of the individual elements should not overcome 5% of their nominal value according to the ASTM quality standards for Nb alloys [7].

To solve such technical limitations, former works investigated the use of different manufacturing methods, including vapour deposition [6], powder metallurgy [2, 8, 9], ingot casting plus thermomechanical processing [6, 8] and arc melting [3, 9]. Jéhanno *et al.* [8] employed a powder metallurgical processing route combined with ingot casting to manufacture a Nb-24Ti-20Si-5Cr-3Hf-2Al alloy. The variation of its chemical composition is reported in Table 1, where the deviation of the individual elements is normalized with respect of their target in the form $c_{\text{normalized}} = (\text{experimental value} - \text{target})/\text{target}$: as Hf and Al perfectly reach their concentration, Nb, Ti and Si miss their target values with reasonable tolerance, (*i.e.* -2.21% to +0.85%), while the concentration of Cr is significantly above its target, (*i.e.* +7.2%). Drawin *et al.* [2, 9] manufactured several samples of the Nb-25Ti-8Hf-2Al-2Cr-16Si alloy alternatively by powder metallurgy (hot extrusion), ingot casting and arc melting. The normalized deviation from the targeted chemical composition reported in Table 1 evidences a homogeneous concentration for Nb, tolerable deviation for Ti from its target, but marked variations for Hf, Cr, Al and Si, with values between -6.25% and 10%. Bewley *et al.* [6] and Gang *et al.* [3] obtained homogenous casts without gross segregation through the hybrid combination of several technologies, (*i.e.* vapour deposition, ingot casting and arc melting) and a minimum of five remelting steps for the same sample. The alloying route of the samples started from buttons of the pre-alloyed Nb-MASC compound manufactured by arc melting.

Alternatively to the cited methods, this work proposed uniquely the employment of the induction cold crucible furnace (ICCF): the generation of strong electromagnetic (EM) forces inside the charge results in the semilevitation effect, a partial detachment of the melt from the crucible’s wall which minimizes their mutual contact. At the same time, the cooling of the crucible generates a solid fraction inside the melt (the so-called “skull”)

Table 1. Variation of the chemical composition of formerly-manufactured Nb-MASC alloys (in %). All values are normalized to their target composition.

	Nb	Ti	Si	Hf	Cr	Al
Jéhanno <i>et al.</i> [8]	+0.85	-2.21	-1.15	0	+7.20	0
Drawin <i>et al.</i> [2, 9]	+0.43	+1.6	-6.25	-5	+10	-5

which, beside the semilevitation, avoids the formation of impurities inside the liquid charge and protects the crucible from any chemical aggressiveness. Furthermore, the liquid material benefits of intense stirring, fundamental for the mixing of multicomponent alloys.

With the ICCF, the main objective of this work is to achieve a more simple manufacturing route in comparison to the ones already tested. Contemporary, the study was aimed to select the suitable EM inputs and to design the TH conditions necessary to realize a reproducible induction melting process for Nb-MASC alloys, potentially based uniquely on the employment of the ICCF. Finally, the homogeneity of the targeted Nb-MASC alloy was aimed to be maximized with the minimum number of remelting steps for the same charge.

The manufacturing process was investigated for two compounds: the binary, eutectic Nb-18Si, and the six-component Nb-16Si-22Ti-4Cr-3Al-2Hf, from now on, referred to as the “full Nb-MASC compound”. Both of them were provided by the Institut für Werkstoffkunde. Because of their multicomponent nature, the manufacture of the latter was constrained by the accomplishment of a highly-homogeneous alloy for the former.

The design of the induction melting process developed in this work was based on three main steps: as first, the analytical estimation of the suitable melting conditions; the second step consisted in the experimental tests, and the final one was the chemical analysis of the solidified alloy, aimed to measure the chemical composition and the internal homogeneity of its elements. The reproducibility of the melting process and the optimization of the alloying were investigated with a multivariable approach, based on the variation of the following parameters:

- The total volume of the charged compound, with the goal to maintain stable hydrodynamic (HD) and thermal (TH) conditions during the melting process, especially during the semilevitation of the melt. With this purpose, the investigation was carried out for two volumes of the charge, 100 cm^3 and 130 cm^3 , selected by the authors in former works on the basis of a computational optimization.

- Dimensions and alloying conditions of the elements charged in the ICCF and employed for the melting. At the beginning of the work, it was proposed to employ solid pellets of the individual elements with different dimensions and equivalent diameter between 5 and 10 mm, the most easily available on the market. Alternative options would have been pre-alloyed buttons, or even pre-alloyed cylindrical blocks of the compound with different diameters.

- Electrical inputs of the induction melting process, like frequency and supplied power, aimed at maximizing both the chemical homogeneity in the charge and the efficiency of the melting.

- Effect of the melting atmosphere on the charge.

- Number of melts necessary to homogenize the charge and the effect of the EM forces on the final concentration of all elemental components.

To quantify the quality of the alloy, the chemical concentration of each elemental component was measured at four points inside the manufactured sample after cutting it along its diameter with the erosion machine, as shown below in Fig. 4: three points were located along the vertical axis, while the last one was placed near the surface of contact between the melt and the cold crucible. Exact locations of the measurement points are reported in Table 2. Besides the individual concentration of all elements, normalized variations from their target values were averaged and compared with the former works by Drawin *et al.* [2, 9], Gang *et al.* [3], Bewlay *et al.* [6] and Jéhanno *et al.* [8].

Table 2. Coordinates of the points for the chemical concentration measurement. The origin of the reference system is located at the bottom of the sample, along its vertical symmetry axis.

	Measurement point (MP)			
	MP1	MP2	MP3	MP4
X [mm]	0	19	0	0
Y [mm]	32	32	2	73

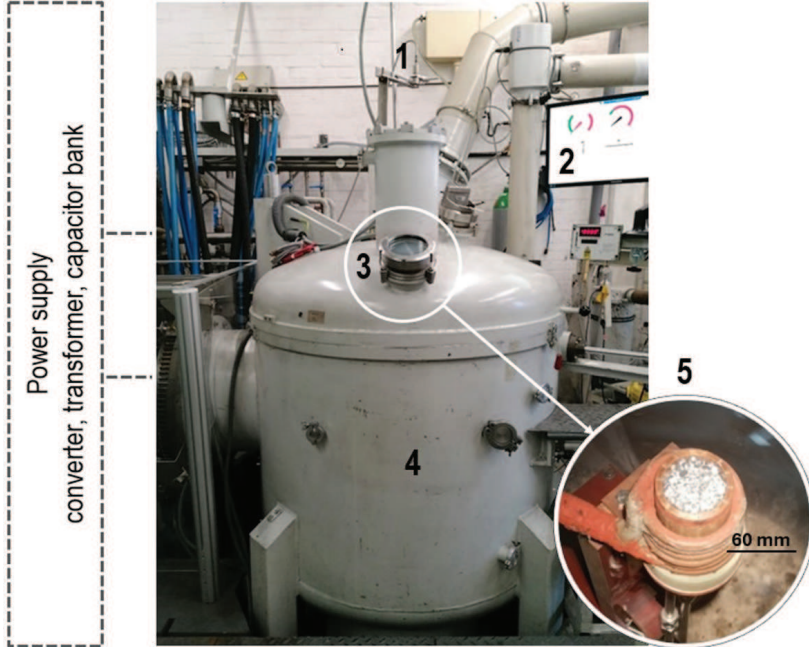


Fig. 1. Experimental setup employed for the induction melting in the ICCF: (1) two-colour pyrometer, (2) monitoring computer, (3) protective glass, (4) protective chamber and (5) induction cold crucible furnace with the corresponding inductor and the charge.

2. Design of the induction melting setup for Nb-MASC alloys.

The melting setup used for the study was a laboratory-scale induction cold crucible furnace with internal volume of 282 cm³. The setup, visible in Fig. 1, is installed at the Institute of Electrotechnology of the Leibniz University Hannover, inside a protective chamber, where either vacuum atmosphere (approximately 6 · 10⁻⁵ bar) or argon could be injected at a pressure of 0.3 bar. Electric power was supplied by an EMA-TEC converter with the maximum power of 300 kW. To measure the temperature at the surface of the melt, a two-colour pyrometer was installed above the chamber. The operating frequency for the induction melting process was chosen on the base of the equation [10]

$$f_{\text{opt}} \geq \frac{m^2}{d_{\text{wp}}^2 \sigma_{\text{wp}} \pi \mu_0}, \quad (1)$$

where d_{wp} (m) is the diameter of the charged material, σ_{wp} (S/m) its electrical conductivity and $\mu_0 = 4\pi \cdot 10^{-7}$ H/m is the vacuum magnetic permeability (since no magnetic

materials are involved). The dimensionless coefficient $m = d_{\text{wp}}/\delta$ depends on the EM penetration depth δ (m) and quantifies the quality of the EM coupling between the charged workpiece and the EM field. As reported by Nacke *et al.* [11], Kudryash [12] and Bernier [13], the maximum amount of the power density induced inside the workpiece is ensured for ratios $d_{\text{wp}}/\delta = 2.5\text{--}5$. The presence of multiple elements with dissimilar properties makes an optimal design of the melting process more complex, as they are not characterized by uniform conditions. To find a compromise between all charged materials, the study accounted for some assumptions: the electrical conductivity of the charge was considered for the full Nb-MASC compound, with the value of $\sigma_{\text{el}} = 3.267 \text{ MS/m}$ reported by Samsonov [14]. For the melting of pellets, the average equivalent diameter of $d_{\text{wp}} = 7.5 \text{ mm}$ was taken. Assuming the ratio $d_{\text{wp}}/\delta = 5$, Eq. (1) returns the optimal frequency of $f_{\text{opt}} = 10.97 \text{ kHz}$. This was set at the generator to perform the melting process. It must be cited that other studies report the value of $\sigma_{\text{el}} = 1.39 \text{ MS/m}$ [15–17], which still results in the EM coupling of $d_{\text{wp}}/\delta = 3.25$ at the same frequency.

The melting power supplied by the generator was calculated using the formula

$$P_{\text{gen}} = \frac{P_{\text{wp}}}{\eta_{\text{el}}} \quad (2)$$

prior to the numerical computation of the crucible’s efficiency, respectively, for the volume of 100 cm^3 , equal to $\eta_{\text{el}} = 0.288$, and the 130 cm^3 volume, $\eta_{\text{el}} = 0.30$. The amount of power induced within the charge to reach its melting temperature is calculated from

$$P_{\text{wp}} = \frac{\Delta\theta_{\text{wp}}}{R_{\text{th}}}, \quad (3)$$

with $\Delta\theta_{\text{wp}} = \theta_{m,\text{wp}} - \theta_0$ corresponding to the temperature difference between the melting point of the charge $\theta_{m,\text{wp}}$ and its initial temperature $\theta_0 = 20^\circ\text{C}$, and $R_{\text{th}} = 0.12 \text{ K/W}$ being the thermal resistance of the cold crucible already calculated in former works by Turewicz [18] and Vogt [19]. This accounts for the thermal losses by conduction between the solid fraction of the charge and the crucible’s bottom, and includes an estimation of the thermal losses by radiation from the free surface of the melt.

2.1. Melting and alloying of Nb-18Si in vacuum atmosphere. The melting process for the binary compound was carried out starting from solid pellets of the two elemental components. In the frame of a simplification of the melting route, the use of pre-alloyed materials was not considered in this phase of the work, and the process was performed under the vacuum atmosphere of approximately 10^{-5} bar. Pellets were displaced on the horizontal layers inside the cold crucible, alternated along the axial direction, to promote their mixing during the alloying phase. To start, a total volume of 100 cm^3 was chosen for the compound, corresponding to 35.5% of the total volume of the crucible. To maintain control on the melting process and the resulting semilevitation of the liquid material, the power supplied by the generator was progressively increased every 90 seconds in equal steps of 5 kW each, also necessary to avoid rapid thermal stress to the cold crucible. The melting point of the binary alloy is reported at $\theta_{m,\text{wp}} = 1916^\circ\text{C}$ [6], and Eq. (2) returns the supplied power of $P_{\text{gen}} = 55.4 \text{ kW}$.

Experiments proved a good predictability of the process, with the melt completely liquid at 50 kW, as multiple pellets started to melt already at 40 kW, very probably silicon. Once stable TH and HD conditions were achieved, the measured temperature on the melt surface was 2040°C . In Fig. 2 the charging and the melting processes of the binary alloy are shown, together with the cast obtained after the solidification inside the

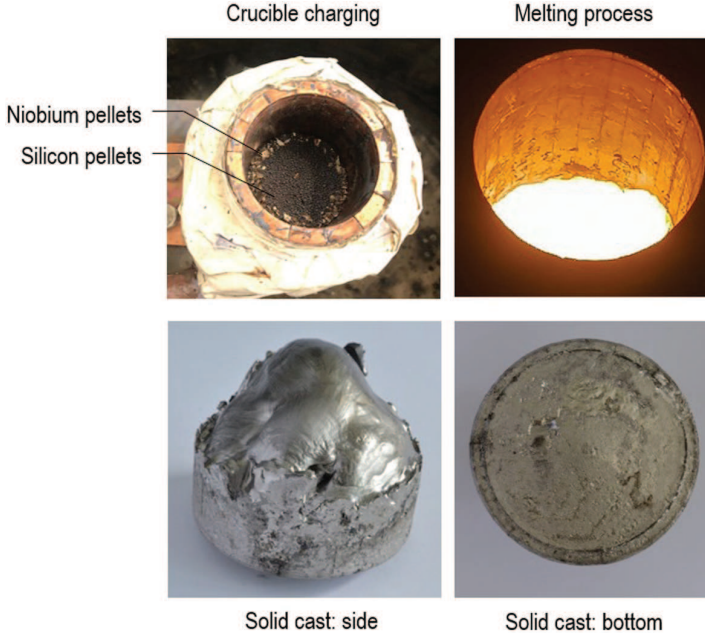


Fig. 2. Induction melting process and experimental result for the binary alloy Nb-18Si.

cold crucible. The picture on the right evidences of the deformation of the free surface of the charge due to the pinching effect and the semilevitation melting by the EM forces. As for the most relevant results, it was observed that the meniscus maintained a stable deformation during the melting process. Chemical analysis performed at the measurement points inside the manufactured alloy reported average concentrations of 83.7 at.% for Nb and 17.4 at.% for Si, corresponding to normalized deviations of respectively +2.1% and -3.3% from the targeted composition. Both values indicate excellent homogeneity of the alloy manufactured with a single melt, as it fully complies with the ASTM quality standards.

2.2. *Melting and alloying 100 cm³ of full Nb-MASC in vacuum atmosphere.* One of the major limits in the manufacture of the full Nb-MASC compound employed in this work was the very low amount of information about its thermodynamic properties. For compounds with similar chemical compositions, the literature reports the melting point of 1840°C [14]. It turns that the estimated power to be supplied for the melting process amounts to $P_{\text{gen}} = 51 \text{ kW}$, with $P_{\text{wp}} = 15.3 \text{ kW}$ induced in the workpiece.

On the basis of the previous experiment, a first melting and alloying process for the full Nb-MASC compound was carried out in the following conditions: all elemental components were charged in the crucible in the form of solid pellets, displaced with the criteria of increasing mass density – from low-density materials at the bottom of the crucible to the high-density ones at the top. With the help of the EM forces and the strong turbulence of the melt flow such strategy was expected to enhance the mixing between all components. Again, the process took place in vacuum atmosphere and the supplied power was progressively increased in steps of 5 kW each.

During the experiments, the generation of the liquid fraction occurred between 45 and 50 kW, at the measured temperature of 1835°C, confirming the melting point reported in the literature and the good predictability of the analytical calculation for the

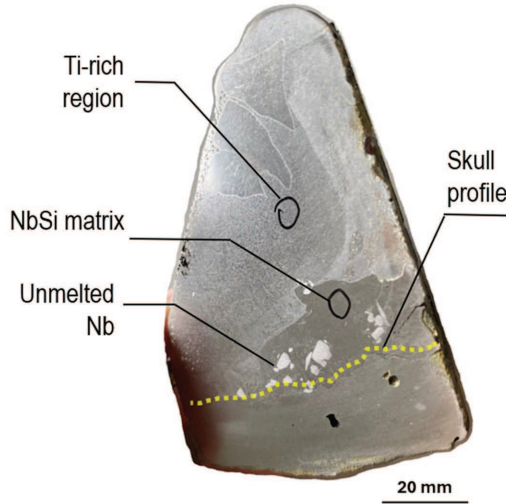


Fig. 3. Experimental result of the induction melting and alloying process for the full Nb-MASC compound with 100 cm³ volume: internal view of a cut solidified cast.

supplied power. Aside the good predictability of the melting effects, other factors influenced the alloying process which could not be considered before: as visible in Fig. 3, the manufactured alloy evidenced of incomplete mixing with a major fraction of Ti, corresponding to 70 at.%, concentrated in the upper volume of the solid cast (light-grey zone in the figure). Only the remaining 30 at.% was distributed in the lower part. Unmelted pellets of Nb were still present, denoting an incomplete dissolution and alloying with the compound. The formation of the Nb-silicide matrix was visible in a minor portion of the alloy (dark grey in the figure), where though Hf mixed with tolerable homogeneity. A crucial issue with the formation of the alloy is concerned with the evaporation of the low-melting components, Al and Cr. Chemical analysis reported evaporation effects equal to 73 at.% for Al and to 92.5 at.% for Cr. Such effect can be explained by the employment of vacuum atmosphere for the melting process and can be analytically proved by the Clausius–Clapeyron equation:

$$T_B = \left(\frac{1}{T_0} - \frac{R \ln(P/P_0)}{\Delta H_{\text{vap}}} \right)^{-1}. \quad (4)$$

The boiling point T_B can be expressed as a function of the absolute pressure, where T_0 [K] is the boiling pressure of a medium at the atmospheric pressure P_0 [Pa], $R = 8.134 \text{ J}/(\text{K}\cdot\text{mol})$ is the universal gas constant and ΔH_{vap} [J/mol] is the heat of vaporization of the liquid. At the absolute pressure of $6 \cdot 10^{-5}$ bar used in the experiment the boiling point of Al corresponds to 1287.3°C and the one of Cr is 1467.1°C. Both are much lower than the temperature at which the melting process occurs. Finally, minor instabilities of the melt meniscus were observable during the melting process caused by the action of the EM forces.

2.3. *Melting and alloying 130 cm³ of full Nb-MASC in argon atmosphere.* To solve the issues encountered in the previous experiments, the melting conditions for the full compound were modified in the following way:

- The volume of the charge was scaled up to 130 cm³ to reduce the deformation of

the melt and contemporary increase the manufactured amount of material (corresponding now to 46% of the crucible's volume).

- Argon gas was injected into the protective chamber with the main aim to increase the operating pressure up to 0.3 bar and contemporary avoid oxidation. According to Eq. (4), at the corresponding pressure the boiling points of Al and Cr are, respectively, 2230.2°C and 2437.4°C, much higher than the melting temperature at which the process is conducted. No risk of evaporation was expected that time.

- The melting process for the same charge was proposed to be conducted twice, after being turned upside down inside the crucible, to promote the transport of the elements and enhance their homogenization inside the melt.

- As the unmelted pellets of Nb represented a crucial issue for the quality of the manufactured alloy, at this step, different electrical conditions necessary to achieve their complete melting were tested.

Under the frequency of 10.9 kHz, maximum power supplied by the generator was increased to $P_{\text{gen}} = 75 \text{ kW}$. This corresponded to the value necessary to reach the melting point of niobium, (*i.e.* 2477°C [6]) on the basis of Eq. (3) and Eq. (2). Furthermore, the melting process was carried on for additional 5 minutes after the achievement of the liquid phase to promote supplementary stirring inside the melt.

As seen in Fig. 4, the homogeneity of the alloy improved significantly in comparison to the former experiments: the melt showed a stable meniscus and no evaporation of any

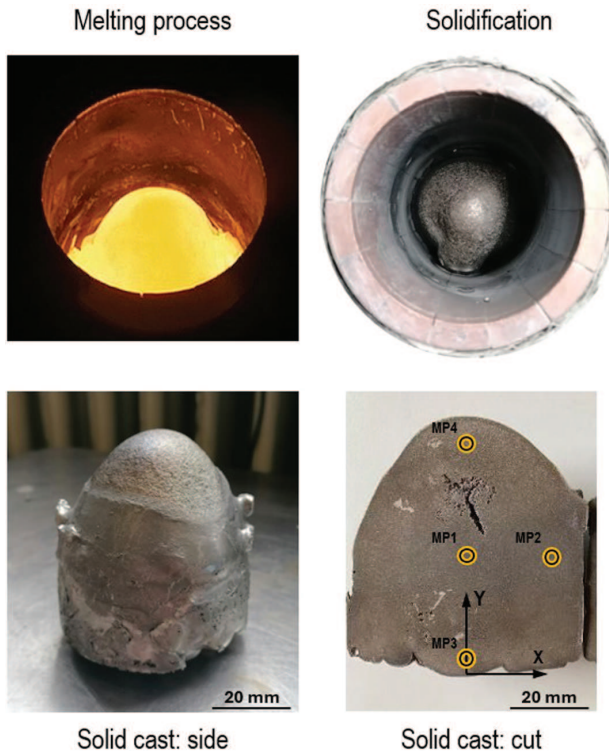


Fig. 4. Induction melting process and experimental result for the full Nb-MASC compound with 130 cm³ compound. The internal view of the cut solidified cast is visible in the bottom-right picture.

Table 3. Variation of the normalized chemical composition of the full Nb-MASC alloy manufactured in this work (in %). All values are averaged between the measuring points and are normalized to their target.

	Nb	Ti	Si	Hf	Cr	Al
Nb-18Si compound	+2.1		-3.3			
Full Nb-MASC compound	-3.4	+1.6	+4.1	-17.7	+3	+34.8

element was reported. Chemical concentrations of its elemental components have been published in former works by the authors [20, 21] and count a maximum variation of 2.2 at.% of the targeted value in the case of Nb. The average values of the normalized deviations are listed in Table 3: with a deviation lower than 5% from their nominal composition, Nb, Ti, Si and Cr still satisfy the ASTM homogeneity standards. On the contrary, Hf and Al show much higher deviations of respectively -17.7% and 34.8% outside the tolerance of the accounted regulations.

Conclusion.

Induction melting in the cold crucible furnace was tested to manufacture Nb-MASC compounds and contemporary to solve the technical complexities related to their alloying.

Through the variation of the melting conditions, the melting process in ICCF was optimized for compounds made of up to six elements, for the maximum volume of the charge corresponding to 130 cm³. For the two tested compounds, Nb-18Si and Nb-16Si-22Ti-4Cr-3Al-2Hf, suitable alloying conditions were found in the charging of solid pellets of the individual elements, placed in targeted locations inside the crucible. Melting of the binary Nb-18Si was successful in vacuum atmosphere, and a single melting was sufficient to guarantee high homogeneity of the sample, above the industrial quality standards. On the other hand, the alloying route of the full Nb-MASC alloy required a more complex strategy, as protecting atmosphere in Ar gas was crucial to avoid the evaporation of the elements with the lowest melting temperature, (*i.e.* Al and Cr). In addition, chemical homogeneity was promoted with the double melting of the same sample and longer melting times, up to 17 minutes for each charge (excluding the additional solidification time of 30 minutes inside the crucible). The chemical concentration of the full Nb-MASC alloy was affected by minor non-homogeneities of two elements, (*i.e.* Al and Hf), which sets its homogeneity below the industrial quality standards. On the basis of the results obtained in this work, such issues are expected to be solved in future researches through the application of higher melting power and additional melting steps of the same charge in the ICCF.

Aside such minor non-homogeneities in the full Nb-MASC compound, this study demonstrates how its melting process in ICCF is fully controllable and reproducible. The employment of a unique technology and the characterization of the suitable alloying conditions supported by analytical calculations provide significant improvements for the multi-technology manufacturing strategies tested until now.

This opens the process up to the potential scalability to industrial-scale ICCFs and its application in aviation for the production of blades for energy-efficient turbines. Future advances of this research aim at the implementation of directional solidification for complex Nb-MASC compounds to be performed in the cold crucible furnace after the phases of melting and alloying. This would guarantee the production of blades character-

ized by mechanical properties comparable to the ones made with Ni-based superalloys.

Acknowledgments.

The development of this study was funded by the *Deutsche Forschungsgemeinschaft* (DFG, German Research Foundation). Authors express their gratitude for the support under grant No. BA 3565/5-1.

References

- [1] I.A. ESSIENUBONG, O. IKECHUKWU, P.O. EBUNILU AND E. IKPE. Material selection for high pressure (HP) turbine blade of conventional turbojet engines. *American Journal of Mechanical and Industrial Engineering*, vol. 1 (2016), no. 1, pp. 1–9.
- [2] S. DRAWIN AND J.F. JUSTIN. Advanced lightweight silicide and nitride based materials for turbo-engine applications. *AerospaceLab*, vol. 3 (2011), pp. 1–13.
- [3] F. GANG, A. KAUFFMANN AND M. HEILMAIER. Phase evolution in and creep properties of Nb-rich Nb-Si-Cr eutectics. *Metallurgical and Materials Transactions A*, vol. 49 (2018), pp. 763–771.
- [4] P. TSAKIROPOULOS. On Nb silicide based alloys: alloy design and selection. *Materials*, vol. 11 (2018), no. 5, pp. 844.
- [5] C. SEEMÜLLER AND M. HEILMAIER. Grain boundary sliding-induced creep of powder metallurgically produced Nb-20Si-23Ti-6Al-3Cr-4Hf. *Materials Transactions*, vol. 59 (2018), no. 4, pp. 538–545.
- [6] B.P. BEWLAY, M.R. JACKSON, J.-C. ZHAO AND P.R. SUBRAMANIAN. A review of very-high-temperature Nb-silicide-based composites. *Metallurgical and Materials Transactions A*, vol. 34 (2003), no. 10, pp. 2043–2052.
- [7] Standard Specification for Niobium and Niobium Alloy Ingots, ASTM B391-18. (ASTM International, 2018.)
- [8] P. JÉHANNO, M. HEILMAIER, H. KESTLER, M. BÖNING, A. VENSKUTONIS, B. BEWLAY AND M. JACKSON. Assessment of a powder metallurgical processing route for refractory metal silicide alloys. *Metallurgical and Materials Transactions A*, vol. 36 (2005), no. 3, pp. 515–523.
- [9] S. DRAWIN, J. P. MONCHOUX, J.L. RAVIART AND A.. COURET. Microstructural properties of Nb-Si based alloys manufactured by powder metallurgy. *Advanced Materials Research*, vol. 278 (2011), pp. 533–538.
- [10] F. BENEKE, B. NACKE AND H. PFEIFER. *Handbook of Thermoprocessing Technologies*. (Vulkan Verlag, Essen, 2015).
- [11] B. NACKE AND E. BAAKE. *Induction Heating*. (Vulkan Verlag, Essen, 2016).
- [12] M. KUDRYASH. Experimental Investigation of Induction Melting in Cold Crucible for High Temperature Processing of Oxides Using HF Transistor. PhD Thesis, Leibniz University Hannover, 2011.
- [13] F. BERNIER. Optimierung des thermischen Verhaltens metallischer Schmelzen im Kaltwand-Induktions-Tiegelofen. PhD Thesis, Leibniz University Hannover, Hannover, 2001.

- [14] P.R. SUBRAMANIAN, M.G. MENDIRATTA, D.M. DIMIDUK AND M.A. STUCKE. Advanced intermetallic alloys – beyond gamma titanium aluminides. *Materials Science and Engineering: A*, vol. 239-240 (1997), pp. 1–13.
- [15] M.G. MENDIRATTA, J.J. LEWANDOWSKI AND D.M. DIMIDUK. Strength and ductile-phase toughening in the two-phase Nb/Nb₅Si₃ alloys. *Metallurgical Transactions A*, vol. 22A (1991), pp. 1573–1583.
- [16] M.G. MENDIRATTA AND D.M. DIMIDUK. *Metallurgical Transactions A*, vol. 24A (1993), pp. 501–504.
- [17] J.D. RIGNEY AND J.J. LEWANDOWSKI. *Metallurgical Transactions A*, vol. 27 (1996), pp. 3292–3306.
- [18] P. TUREWICZ. Multiphysikalische Prozessanalyse zur Erweiterung der Einsatzgrenzen des Kaltwand-Induktions-Tiegelofens. PhD Thesis, Leibniz University Hannover, 2013.
- [19] M. VOGT. Einsatz des Kaltwand-Induktions-Tiegelofens zum Schmelzen und Gießen von TiAl-Legierungen. PhD Thesis, Leibniz University Hannover, 2001.
- [20] M. GUGLIELMI, E. BAAKE, A. KÖPPEN, E. HOLZMANN AND S. HERBST. Induction melting in a cold crucible furnace applied to innovative high-melting temperature materials. *Magnetohydrodynamics*, vol. 58 (2022), no. 4, pp. 523–532.
- [21] M. GUGLIELMI, E. HOLZMANN, A. KÖPPEN, E. BAAKE, AND S. HERBST. Investigation of an alloying process for NbSi-based composites in cold wall crucible furnace. In: *Proc. the HES-23 International Conference on Heating by Electromagnetic Sources*, (Padua, Italy, May 10–12, 2023.)

Received 29.11.2024